Generalized algorithm for efficient multi-channel data fusion and real-time implementation using wavelet transform

Viraj K. Mehta, Hamid Krim
North Carolina State University
Raleigh, NC 27695

***Abstract*-This paper presents an approach to efficient real-time fusion of multi-channel remote sensing data using sparseness generated by wavelet transform. The experimental data used is from the SSM/I (Special Sensor Microwave/Imager) instrument. Starting with a general Bayesian estimation formulation of the problem to generate an enhanced resolution field we apply a wavelet transform that yields a reduction in computation costs without compromising on quality of fused data. The approach hinges on preconditioning the required field into having white statistics. We subsequently apply filters to the input channels to cast them in a common basis where they may be combined by simple addition of coefficients. The reconditioning of this data produces the ultimately desired field.**

I. Introduction

In [5] we have introduced a Bayesian estimation approach to data fusion of multiple channels of SSM/I instruments [3]. We emphasized the application of a pre conditioning whitening transform that led to a simplified choice of a wavelet transform with a resulting sparseness of representation. Mathematically, Eq. (1) represents the solution to Bayesian estimation with $\mathbf{X}$ denoting the underlying field being estimated, $\mathbf{G}$, the Gain of the measurement antenna, and $\mathbf{Y}$ denoting the observed measurements, and $\mathbf{P}$ and $\mathbf{R}$ representing the covariance matrices of $\mathbf{X}$ and measurement error $\mathbf{E}$ respectively. Applying the whitening and wavelet transforms yields Equation (2) for estimation, where $\mathbf{X}_l = \mathbf{W}_l\mathbf{F}_W\mathbf{X}$, $\mathbf{G}_l = \mathbf{G}\mathbf{F}_W^{-1}\mathbf{W}_l^T$, $\mathbf{P}=\mathbf{A}\mathbf{A}^T$ (where $\mathbf{A}$ is a full rank Upper Triangular matrix) and $\mathbf{F}_W = \mathbf{A}^{-1}$.

$$\hat{\mathbf{X}} = (\mathbf{P}^{-1} + \mathbf{G}^T\mathbf{R}^{-1}\mathbf{G})^{-1}\mathbf{G}^T\mathbf{R}^{-1}\mathbf{Y}, \tag{1}$$

$$\hat{\mathbf{X}}_l = \mathbf{W}_l\mathbf{F}_W\hat{\mathbf{X}} = (\mathbf{I} + \mathbf{G}_l^T\mathbf{R}^{-1}\mathbf{G}_l)^{-1}\mathbf{G}_l^T\mathbf{R}^{-1}\mathbf{Y}\,. \tag{2}$$

$\mathbf{W}_l$ is the 2D Haar wavelet transform which preserved the low frequency portion of the level-1 decomposition. This yields tremendous storage savings due to the compact representation. In this paper we propose a generalization of this technique to any multispectral data with appropriate assumptions on the statistics and data formatting pertaining to the instrument of interest. We also show a real-time implementation for the above formulation for data from two channels of the SSM/I instrument that is based on filtering each of the input channels individually to generate data in a common basis where fusion is accomplished by addition of coefficients.

II. Statistical Analysis and Formulation

Every input channel for an instrument will correspond to data from a 2 dimensional grid and the first step in the formulation is to vectorize the input data into a 1-D column vector, i.e. $\mathbf{Y}_1$=Vec[2D channel-1 data]. We carry out simple vectorization and append various channel data to the same column vector data as $\mathbf{Y}=[\mathbf{Y}_1, \mathbf{Y}_2, \ldots]^T$ where $\mathbf{Y}_1$, $\mathbf{Y}_2\ldots$ are the vectorized measurements of each channel. At the same time we need an assumption on the fineness of the field to be estimated i.e. $\mathbf{X}$. This should be based on desired resolution and achievability based on spatial dependencies in the input data. In general, the greater the spatial dependencies (overlap) in the input data the more resolved should be the grid of the estimated data. For our experiments with the SSM/I data we used a grid finer by 4 times in each dimension than the finest input data available (85GHz [3]).

To model the antenna gain operator $\mathbf{G}$ the actual antenna gain pattern should be taken into consideration. For the SSM/I instrument we found that a jointly binomial gain pattern over the channel footprints was a sufficiently accurate model. Suitably formatting the gain matrix for multiple channels and vectorized data yield the mathematical operator $\mathbf{G}$.

We then need to empirically estimate the *a priori* covariance matrices $\mathbf{P}$ and $\mathbf{R}$ of the field $\mathbf{X}$ and the error in measurement $\mathbf{E}$ respectively. Here we lay emphasis on measurement of covariance statistics for a row of pixels to be estimated and corresponding generation of $\mathbf{P}$ using assumptions of isotropy. For the SSM/I instrument we were able to fit the empirical statistics to an exponential model (3) [5]. The model is subsequently used to generate the appropriately formatted matrix $\mathbf{P}$ as given by (4) for a swath width N in terms of the underlying pixels.

$$C(d) = A \cdot \exp(B \mid d \mid), \tag{3}$$

$$\begin{aligned} P(x,y) = C(d) = \\ = C(\sqrt{(\lfloor x/N \rfloor - \lfloor y/N \rfloor)^2 + (x - \lfloor x/N \rfloor - y + \lfloor y/N \rfloor)^2} \\ = A \cdot \exp\{-B \\ \cdot \sqrt{(\lfloor x/N \rfloor - \lfloor y/N \rfloor)^2 + (x - \lfloor x/N \rfloor - y + \lfloor y/N \rfloor)^2}\} \end{aligned} \tag{4}$$

Even though, the method outlined here for determining **P** is specific to the SSM/I instrument, several key points may be generalized. For any given instrument, the corresponding process would involve the following steps:

- Observe characteristics of sample data to determine what input channel(s) provide statistical data that is closest to the underlying field and thus has minimum overlap.
- Apply statistical modifications (e.g. local mean removal) to selected data to guarantee the imposed assumptions of stationarity.
- Compute the covariance matrix for the relevant input data points.
- If possible, fit this covariance matrix with a mathematical model.

From the generated model, develop the final form that is adapted to the vectorized field with a specified swath length.

The measurement error **E** in every channel is assumed to be zero mean additive white gaussian noise. Assuming non-correlation and equal variance for one channel, the error covariance matrix is just $\sigma^2\mathbf{I}$ for each of the channels, where σ is the standard deviation for measurement errors in that channel.

We can have different error variances for different channels. Ideally, one would like to determine empirical estimates of the error variance for subsequent computations. In the absence of dependable empirical results we may however interpret the error variance as a weighting factor. In other words, by selecting higher error variance for a particular channel we are estimating our underlying field to a lesser extent from it. This turns out to be very useful in the SSM/I setting. Since, the lower resolution channels give us less accurate measurements then the higher ones, we might want to derive our estimation more from the higher resolution channels than the lower ones. This leads us to selecting $\sigma_4^2 > \sigma_3^2 > \sigma_2^2 > \sigma_1^2$ for 4 input channels with channel 1 being the one with highest resolution, where the terms are the measurement error variances of the respective channels.

Note that this still does not provide us with an exact method to determine the individual channel measurement error variances, but merely imposes constraints. We thus have to empirically and a bit qualitatively select them. The final Covariance Matrix **R** is thus diagonal with elements of the diagonal being the variance of the measurement error for the channel that the measurement corresponds to, i.e.,

$$\mathbf{R} = \begin{bmatrix} \sigma_1^2 I_{n^2 x n^2} & 0 & 0 & 0 \\ 0 & \sigma_2^2 I_{n^2/4 x n^2/4} & 0 & 0 \\ 0 & 0 & \sigma_3^2 I_{n^2/4 x n^2/4} & 0 \\ 0 & 0 & 0 & \sigma_4^2 I_{n^2/4 x n^2/4} \end{bmatrix} \quad (5)$$

Note that all the zeros in the above matrix indicate that there is no correlation between measurement errors of various channels. Each of the individual error covariance matrices for individual channels contributing to the above matrix is different in size. This is due to the measured data for the underlying field, which depends on *n* that is the width of the local square patch under observation.

III. Real-time Implementation

A. Input grid modification

We now proceed to develop a real-time implementation of the optimized estimation formulation. The focus of the work here is to develop a real-time implementation for the portion $\mathbf{M} = (\mathbf{I} + \mathbf{G}_l^T \mathbf{R}^{-1} \mathbf{G}_l)^{-1} \mathbf{G}_l^T \mathbf{R}^{-1}$ in (2). The rest is already in the form of a cascade of the inverse wavelet and inverse whitening filters. There exists the possibility of simplification of **M** into de-correlation and combination blocks. The need for de-correlation of input channels arises from the fact that the intermediate quantity to be estimated is white, and the combination is just a restatement of fusion.

To visualize the intuition behind the following manipulations aimed towards achieving a real-time implementation, consider the matrix representation of **M**. The estimation of the intermediate quantity is then just a multiplication of the input with this matrix, i.e. $\mathbf{X}_l = \mathbf{M}\mathbf{Y}$ and the final estimation is achieved by reconditioning this intermediate quantity, i.e. $\mathbf{X} = \mathbf{F}_W^{-1} \mathbf{W}_l^T \mathbf{X}_1$. Fig. 1 shows the **M** matrix for input restricted to the 85V and 37V channels for the SSM/I case. (Note: Throughout this section we use the 85V and 37V channels only for demonstrational purposes. Extension to other channels is straightforward.)

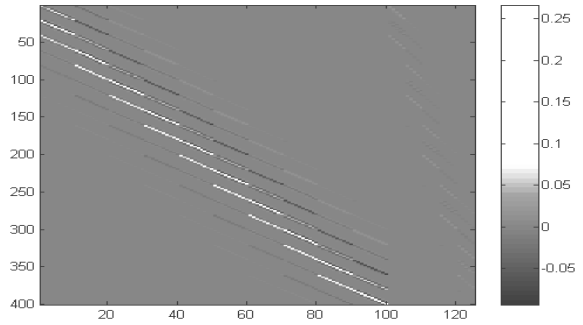

Fig. 1. The M matrix

The dimensions of the **M** matrix shown above are 400x125 for 400 pixels to be estimated for a final field of 1600(40x40) pixels. The first 100 columns indicate operation on the 100 input pixels from a 10x10 field in the 85V channel while the remaining 25 indicate operation on the 25 input pixels from a corresponding 5x5 field in the 37V channel. Thus, the first important conclusion is that we can separate the contributions to a pixel from various input channel as follows:

$$\mathbf{M} = \begin{bmatrix} \mathbf{M}_{85} & \mathbf{M}_{37} & ..... \end{bmatrix}, \tag{6}$$

where $\mathbf{M}_{85}$, $\mathbf{M}_{37}$, … correspond to different channels. The estimation statement follows as:

$$\hat{\mathbf{X}}_1 = \mathbf{M}\mathbf{Y}$$
$$= \begin{bmatrix} \mathbf{M}_{85} & \mathbf{M}_{37} & ... \end{bmatrix} \begin{bmatrix} \mathbf{Y}_{85} \\ \mathbf{Y}_{37} \\ ... \end{bmatrix} = \mathbf{M}_{85}\mathbf{Y}_{85} + \mathbf{M}_{37}\mathbf{Y}_{37} + ... \tag{7}$$

This implies that the operators $\mathbf{M}_{85}$, $\mathbf{M}_{37}$, … can individually de-correlate the input channels, and the estimation of the intermediate preconditioned quantity is then just the addition of the corresponding coefficients for each pixel in the adopted wavelet basis. Let's now consider the portion for the 85V channel first, i.e. the first 100 columns or $\mathbf{M}_{85}$. We notice a certain pattern here. Looking at sets of 10 columns, each column in a set is a vertical shift of its adjoining column by 2 pixels and each set is a vertical shift of the adjoining column by 20 (2x(Swath width)) pixels (one swath is 10 pixels here, since we are estimating from a 10x10 field of the 85V channel). It is now easy to see that our aim of developing a real-time implementation is realized if we carry out some input reformatting that makes every column a vertical shift of the adjoining column by one pixel, i.e. construct a matrix filter to achieve such shifts. This is easily most efficiently accomplished by effectively increasing the 85V channel input sampling rater (to a higher resolution grid

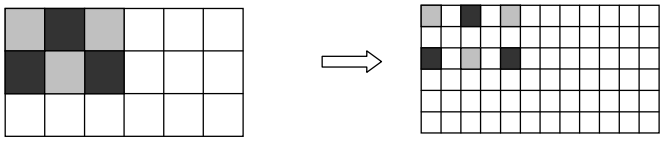

Fig. 2. Pictorial representation of the input modification that leads to a representation of the matrix operator on the input as a filter

corresponding to the quantity to be estimated) by a systematic insertion of zeros. This is pictorially shown in Fig. 2.

A similar grid modification is required for the 37V channel. Given its original lower sampling rate, more zeros are required for it as the 37V channel. With each **M** matrix as a separate filter for each channel, we have a bank of input filters. Let the input data be modified from $\mathbf{Y}_{85}$, $\mathbf{Y}_{37}$, … to $\mathbf{Z}_{85}$, $\mathbf{Z}_{37}$, … by the aforementioned technique. Now the matrices $\mathbf{M}_{85}$, $\mathbf{M}_{37}$, … become $\mathbf{F}_{85}$, $\mathbf{F}_{37}$, …

$$\therefore \mathbf{X}_1 = \mathbf{F}_{85}\mathbf{Z}_{85} + \mathbf{F}_{37}\mathbf{Z}_{37} + ...$$

$$\therefore \mathbf{X}_1 = \mathbf{f}_{85} * \mathbf{Z}_{85} + \mathbf{f}_{37} * \mathbf{Z}_{37} + ... \quad \text{where} \quad * \quad \text{denotes convolution} \tag{8}$$

Thus, $\mathbf{X}_1$ is obtained by filtering $\mathbf{Z}_{85}$, $\mathbf{Z}_{37}$, … by the filters $\mathbf{F}_{85}$, $\mathbf{F}_{37}$, … and adding up the output coefficients. The simplification of the **M** matrix into a bank of filters thus completes the real-time implementation of the optimal

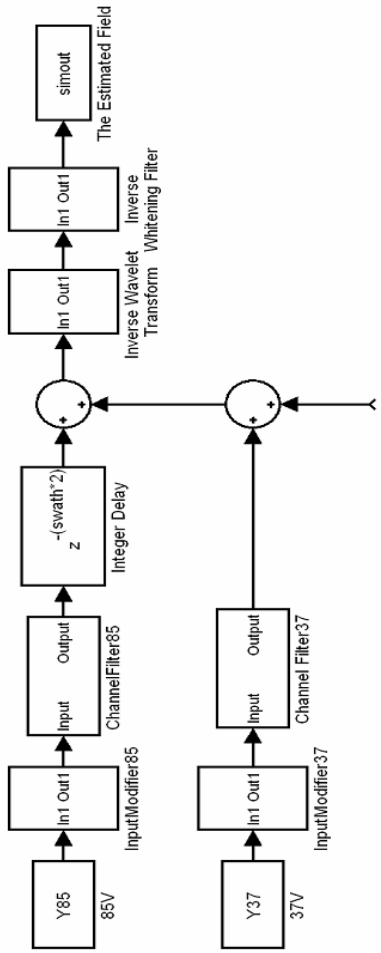

Fig. 3. Block Diagram representation of the real-time implementation of the optimal estimator

estimator.

B. MATLAB simulation experiment

We now proceed to show the exact construction of the real-time implementation. Fig. 3 shows the block diagram representation of such a system. It can easily be extended to include additional channels using a similar approach. On the left hand side is what might be called a bank of filters for the channels. An "input reformatting" block, which carries out the input grid modification as previously explained, precedes every channel filter. To construct a channel filter for say the 85V channel, the first step is to obtain a column of the $\mathbf{M}_{85}$ matrix, which defines the impulse response of the required filter. We can easily construct a Direct Form I FIR filter with the given coefficients of the impulse response. Even though the column length is 400 for our example, the number of

significant values in the impulse response is much smaller, and the resulting filter hence has a compact form. To make the filter independent of the swath width, we observe that the impulse response has significant values in sets of points equivalent to a swath width. The zero values coincide with the middle of any two consecutive sets. This is basically just indicative of the short and long-range dependence of the acquired data on the pixels in the underlying field. For our filter design to be valid for any swath width, we just need to insert zero points between the sets such that the width of the swath still corresponds to the size of the sets. This translates to adding extra delays dependent on swath width between parallel forward paths of the FIR filter. The outputs of the various channel filters are added after accounting for synchronization delays. The sum is then the conditional estimate of the field of interest. The inverse wavelet and "re-coloring" filters applied to this sum yield the final estimate as shown on the right hand side of the block diagram.

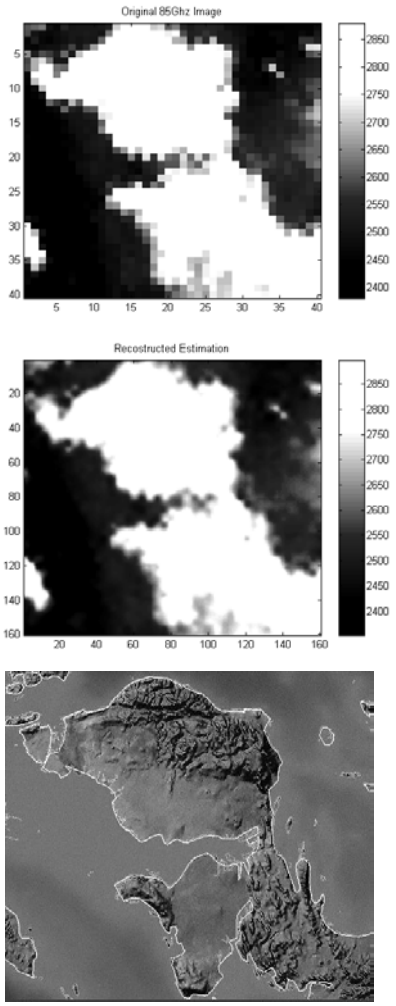

Fig. 4. Comparison of original input 85Ghz data with reconstructed estimation fusion result and geographical map for an area of interest.

IV. Conclusion

The challenges of efficient data fusion and resolution enhancement in satellite imaging have been the driving motivation for this work. We have proposed a real-time Bayesian estimation algorithm consistent with our goals. The evaluations and validations have been carried out on SSM/I data for which we have also developed empirical statistical models.

In all, we have successfully shown the general approach of using compact wavelet representation to gain simplifications in re-configurable hardware for satellite based image processing. While, some of the assumptions specifically pertained to the SSM/I instrument, the proposed approach and methods are sufficiently generic to apply to multispectral remote sensing instruments and thus should prove to be useful.

References

[1] Richard Sethmann, Barbara A. Burns, and Georg C. Heygster, "Spatial Resolution Improvement of SSM/I Data with Image Restoration Techniques," *IEEE Trans. Geosci. Remote Sensing*, vol. 32, no. 6, pp. 1144-1151, 1994.

[2] David G. Long, and Douglas L. Daum, "Spatial Resolution Enhancement of SSM/I Data," *IEEE Trans. Geosci. Remote Sensing*, vol. 36, no. 2, pp. 407-417, 1998.

[3] James P. Hollinger, James L. Pierce, and Gene A. Poe, "SSM/I Instrument Evaluation," *IEEE Trans. Geosci. Remote Sensing*, vol. 28, no. 5, pp. 781-790, 1990.

[4] Wayne D. Robinson, Christian Kummerow, and William S. Olson, "A Technique for Enhancing and Matching the Resolution of Microwave Measurements from the SSM/I Instrument," *IEEE Trans. Geosci. Remote Sensing*, vol. 30, no. 3, pp. 419-429, 1992.

[5] V. K. Mehta, C. M. Hammock, P. W. Fieguth, H. Krim, "Data Fusion of SSM/I Channels using Multiresolution Wavelet Transform," *IEEE International Geoscience and Remote Sensing Symposium (IGARSS)* 2002